Contribution from the Laboratoire de Spectrochimie des Elements de Transition, ERA No. 672, and LURE,[1] Université de Paris-Sud, 91405 Orsay, France, and Laboratoire de Physicochimie Structurale, Université de Paris-Val de Marne, 94000 Creteil, France

EXAFS Structure and Magnetic Properties of a $Cu^{II}Ni^{II}$ μ-Oxalato Mixed Linear Chain

MICHEL VERDAGUER,[2a] MIGUEL JULVE,[2a,b] ALAIN MICHALOWICZ,[2c] and OLIVIER KAHN*[2a]

Received November 17, 1982

The compound $NiCu(C_2O_4)_2 \cdot 4H_2O$ was synthesized. Its X-ray powder pattern is very close to that of $Ni(C_2O_4) \cdot 2H_2O$, with however a characteristic splitting of one of the intense reflections, suggesting an ordered bimetallic chain structure. The EXAFS study on both the copper and the nickel edges at 300 and 30 K is quite consistent with such a structure and may be interpreted as follows: each Cu^{II} has four oxygen atoms and each Ni^{II} has six oxygen atoms as nearest neighbors (Cu-O = 1.96 Å, Ni-O = 2.04 Å). In addition to the atoms of the equatorial oxalato bridges, each Cu^{II} sees two other Cu^{II} atoms belonging to other chains and located at about 4 Å. The theoretical magnetic behavior of coupled $(AB)_N$ ring chains of spins $S_A = {}^1/_2$ and $S_B = 1$ was calculated for $N = 2$-4 and an extrapolation for $N \rightarrow \infty$ was proposed. In the case of antiferromagnetic interaction, the $\chi_M T$ vs. $kT/|J|$ plot for the ordered bimetallic chain exhibits a minimum at $kT/|J| = 0.63$ (8), J being the isotropic exchange parameter of the Hamiltonian $-J\sum_i \hat{S}_i \cdot \hat{S}_{i+1}$. In the range $1 < kT/|J| < 4$, the magnetic susceptibility closely follows the Curie-Weiss law $\chi_M/(cm^3\ mol^{-1}) = 1.444(g^2/4)/(T/K + 1.0467\ |J|/k)$. This theoretical approach was compared to the experimental data. Above 30 K, the magnetic susceptibility of $CuNi(C_2O_4)_2 \cdot 4H_2O$ follows the expected Curie-Weiss law. This allows us to determine $g = 2.16$ (2) and $J = -52.7\ cm^{-1}$. The minimum of $\chi_M T$ vs. T is not observed. This is attributed to the interchain interactions put into evidence in the EXAFS study. Finally, the value of J_{CuNi} in $CuNi(C_2O_4)_2 \cdot 4H_2O$ was compared to those of J_{CuCu} and J_{NiNi} in the homometallic chains copper oxalate and nickel oxalate.

Introduction

A recent communication[3] describing the synthesis, the structure, and the magnetic properties of an ordered bimetallic $Cu^{II}Mn^{II}$ chain opened a new perspective in the field of one-dimensional magnetic systems. However, very great endeavors will be necessary before the physical properties of these systems are thoroughly understood. In particular, there does not exist today any theoretical model to interpret the magnetic properties, except a classical spin approach, the applicability of which is likely limited,[4] and a study on the effect of magnetic and nonmagnetic impurities in linear-chain systems.[5] The simplest one-dimensional ordered bimetallic system with different electronic spins ($S_A \neq S_B \neq 0$) is that with $S_A = {}^1/_2$ and $S_B = 1$. A $Cu^{II}Ni^{II}$ chain would answer this criterion. In this work, we describe the synthesis of such a chain with the oxalato(2-) bridging ligand. We have not been able to grow single crystals, and in order to specify the structure, we use the EXAFS technique at both the copper and the nickel edges. This technique already allowed us to study the structure of the copper(II) oxalate and of the copper(II) chloranilate and bromanilate.[6] We also present the magnetic behavior of the compound in the 1.8-300 K temperature range. The heart of this paper is devoted to the interpretation of these magnetic data. For that, we calculate the theoretical susceptibility of regular rings $(AB)_N$ with $S_A = {}^1/_2$ and $S_B = 1$, and $N = 2$-4, assuming that the interaction between nearest neighbors may be phenomenologically described by the Hamiltonian $-J\hat{S}_A \cdot \hat{S}_B$. This calculation will lead to an approximate value of J in our compound. The meaning of this result and its limitations will be carefully discussed. The J value in the $Cu^{II}Ni^{II}$ system will be compared to the exchange parameters for the two related homometallic chains, namely the copper(II) oxalate and the nickel(II) oxalate.

In this work, we will also describe the structural, magnetic, and EPR properties of the $Cu^{II}Zn^{II}$ chain, in which only one of the metallic ions is magnetic.

Experimental Section

$CuNi(C_2O_4)_2 \cdot 4H_2O$, hereafter denoted $Cu^{II}Ni^{II}$, was obtained as a polycrystalline powder by adding an aqueous solution of nickel(II) perchlorate to an aqueous solution of $K_2Cu(C_2O_4)_2 \cdot 2H_2O$ and $K_2(C_2O_4) \cdot H_2O$ in the respective proportions $1/1/({}^1/_4)$. The presence of potassium oxalate allows us to avoid the precipitation of the homometallic chain $Cu(C_2O_4) \cdot {}^1/_3H_2O$. Anal. Calcd for $CuNiC_4H_8O_{12}$: Cu, 17.16; Ni, 15.85; C, 12.97; H, 2.16. Found: Cu, 16.9; Ni, 15.6; C, 13.13; H, 2.22. The main peaks of the powder X-ray pattern of $Cu^{II}Ni^{II}$ have the following spacing (in Å): 4.77, 3.95, 3.92, 2.96, 2.52, 2.20, 2.06. This pattern is very close to that of the nickel oxalate $Ni(C_2O_4) \cdot H_2O$, with however a quite characteristic splitting of the peak at 3.93 Å. No trace of copper oxalate $Cu(C_2O_4) \cdot {}^1/_3H_2O$ is detectable. The infrared spectra exhibit two ν_{C-O} bands at 1320 and 1360 cm^{-1} characteristic of the μ-oxalato bridges and no $\nu_{C=O}$ band. $CuZn(C_2O_4)_2 \cdot 4H_2O$ is prepared in the same way as $Cu^{II}Ni^{II}$ by replacing nickel(II) perchlorate by zinc(II) perchlorate. However, in contrast to $Cu^{II}Ni^{II}$, where the ratio Cu/Ni is, as expected, very close to 1, the ratio Zn/Cu is around 1.2 in all the samples, suggesting that $CuZn(C_2O_4)_2 \cdot 4H_2O$ is contaminated by some zinc oxalate, $Zn(C_2O_4) \cdot 2H_2O$. Again, the powder X-ray pattern of the $Cu^{II}Zn^{II}$ system is very close to that of zinc oxalate, without any trace of copper oxalate.

EXAFS Study. The X-ray absorption spectra were recorded at LURE,[1] the French synchrotron radiation facility, on the DCI EXAFS spectrometer described by Raoux et al.[8] The data analysis, performed with use of the classical EXAFS formula (phase wave approximation) and the amplitude and phase shifts of Teo et al.,[9] is detailed elsewhere.[10] All the EXAFS spectra were recorded at room temperature and 30 K.

Magnetic Measurements. These were carried out on polycrystalline samples of a few milligrams with a previously described Faraday type magnetometer,[6] equipped with a new continuous-flow cryostat working down to 1.8 K. Independence of the magnetic susceptibility from the

(1) LURE: Laboratoire pour Utilisation du Rayonnement Electromagnétique.
(2) (a) Laboratoire de Spectrochimie des Elements de Transition. (b) Permanent address: Department of Inorganic Chemistry, University of Valencia, Valencia, Spain. (c) Laboratoire de Physicochimie Structurale and LURE.
(3) Gleizes, A.; Verdaguer, M. *J. Am. Chem. Soc.* **1981**, *103*, 7373.
(4) Blöte, H. W. J. *J. Appl. Phys.* **1979**, *50*, 7401.
(5) Imry, Y.; Montano, P. A.; Hone, D. *Phys. Rev. B: Condens. Matter* **1975**, *12*, 253. Hone, D.; Montano, P. A.; Tonegawa, T.; Imry, Y. *Ibid.* **1975**, *12*, 5141.
(6) Michalowicz, A.; Girerd, J. J.; Goulon, J. *Inorg. Chem.* **1979**, *18*, 3004. Verdaguer, M.; Michalowicz, A.; Girerd, J. J.; Alberding, N.; Kahn, O. *Inorg. Chem.* **1980**, *19*, 3271.
(7) Viswamitra, M. A. *Z. Kristallogr., Kristallgeom., Kristallchem., Kristallphys.* **1962**, *117*, 437. Weichert, T.; Lohn, J. *Ibid.* **1974**, *139*, 223.
(8) Raoux, O.; Petiau, J.; Bondot, P.; Calas, G.; Fontaine, A.; Lagarde, P.; Levitz, P.; Loupias, G.; Sadoc, A. *Rev. Phys. Appl.* **1980**, *15*, 1079.
(9) Teo, B. K.; Lee, P. A.; Simons, A. L.; Eisenberger, P.; Kincaid, B. M. *J. Am. Chem. Soc.* **1977**, *99*, 3854.
(10) Teo, B. K. "EXAFS Spectroscopy"; Teo, B. K., Joy, D. C., Eds.; Plenum Press: New York, 1981. Michalowicz, A.; Huet, J.; Gaudemer, A. *Nouv. J. Chim.* **1982**, *6*, 79.

0020-1669/83/1322-2624$01.50/0

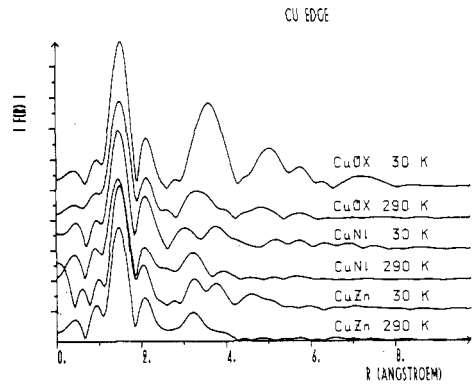

Figure 1. Copper-edge *R*-space Fourier transform spectra at 30 and 290 K, with $|k^3(\chi(k))|$ in arbitrary units vs. *R* in angstroms deduced from experimental data, of $CuC_2O_4 \cdot {}^1/_3H_2O$(*Cu*Ox), $CuNi(C_2O_4)_2 \cdot 4H_2O$ (*Cu*Ni), and $CuZn(C_2O_4)_2 \cdot 4H_2O$ (*Cu*Zn).

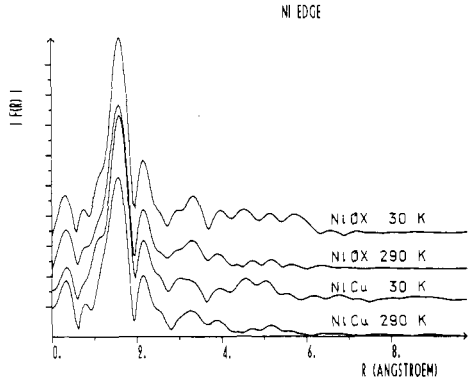

Figure 2. Nickel-edge *R*-space Fourier transform spectra at 30 and 290 K, with $|k^3(\chi(k))|$ in arbitrary units vs. *R* in angstroms deduced from experimental data, of $Ni(C_2O_4) \cdot 2H_2O$ (*Ni*Ox) and $NiCu(C_2O_4)_2 \cdot 4H_2O$ (*Ni*Cu).

magnetic induction was checked at both room temperature and 4.2 K. Mercury tetrakis(thiocyanato)cobaltate(II) was used as a susceptibility standard. Correction for diamagnetism was estimated as -136×10^{-6} cm^3 mol^{-1} for $Cu^{II}Ni^{II}$ and $Cu^{II}Zn^{II}$ compounds.

EPR. The EPR spectra were recorded on powdered samples in the 4.2–300 K temperature range with a Bruker X-band ER 200 D spectrometer equipped with a continuous-flow cryostat. The magnetic field was measured by a Hall probe.

Results and Interpretation of the EXAFS Study

The *R*-space spectra (Fourier transforms of $k^3[\chi(k)]$) of $Cu^{II}Ni^{II}$, $Cu^{II}Zn^{II}$, and homometallic chains copper, nickel, and zinc oxalates are shown in Figures 1–3. Some quantitative results, obtained by least-squares fitting on the first shell M–O, are given in Table I. The accuracy of the M–O bond lengths depends on use of the tabulated phase shifts as universal. The discrepancy between known and EXAFS distances is always found to be less than 0.02 Å. As far as the number of oxygen neighbors is concerned, we did not tabulate the fitted values becaue we did not control accurately the thickness of the samples and therefore the absorption coefficients. However, the values are self-consistent and indicate that the number of oxygen nearest neighbors around nickel (or zinc) is 1.5 times larger than around copper. This agrees with four nearest neighbors around copper and six around nickel (or zinc).

The main conclusions that can be derived from the EXAFS spectra are the following: (i) At 300 K, the first three peaks of all the spectra can be assigned to the M–O, M–C, and M–O′ shells as expected for the bridging network

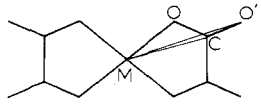

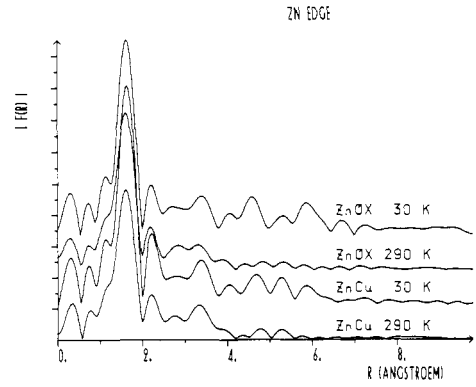

Figure 3. Zinc-edge *R*-space Fourier transform spectra at 30 and 290 K, with $|k^3(\chi(k))|$ in arbitrary units vs. *R* in angstroms deduced from experimental data, of $Zn(C_2O_4) \cdot 2H_2O$ (*Zn*Ox) and $ZnCu(C_2O_4)_2 \cdot 4H_2O$ (*Zn*Cu).

Table I. First-Shell Metal–Oxygen Fitting Results[a]

compd	*T*/K	E_0/eV	*R*/Å	$2\sigma^2$/Å^2	% ρ
	Copper Edge				
$Cu(C_2O_4) \cdot {}^1/_3H_2O$	290	8998	1.98	0.012	1.0
	30	8998	1.97	0.005	2.0
$CuNi(C_2O_4)_2 \cdot 4H_2O$	290	8998	1.96	0.008	3.1
	30	9000	1.96	0.008	3.4
$CuZn(C_2O_4)_2 \cdot 4H_2O$	290	9000	1.95	0.005	2.5
	30	8999	1.96	0.002	2.2
	Nickel Edge				
$Ni(C_2O_4) \cdot 2H_2O$	290	8350	2.04	0.008	1.4
	30	8351	2.04	0.005	1.6
$NiCu(C_2O_4)_2 \cdot 4H_2O$	290	8353	2.03	0.010	1.9
	30	8352	2.04	0.006	1.2
	Zinc Edge				
$Zn(C_2O_4) \cdot 2H_2O$	290	9680	2.08	0.011	2.1
	30	9680	2.09	0.006	2.1
$ZnCu(C_2O_4)_2 \cdot 4H_2O$	290	9680	2.08	0.011	2.5
	30	9680	2.09	0.005	4.1

[a] These parameters are classical in EXAFS analysis: E_0 is the fitted energy edge, *R* is the distance between the absorbing atom and the shell of neighbors, and $2\sigma^2$ is the Debye-Waller factor. The fitting is obtained by nonlinear least-squares refinement and uses the program MINUIT (CERN, version 1973) for the minimization of ρ:

$$\rho = \sum_{k_0}^{k_1} k^5[\chi_{exptl}(k) - \chi_{theor}(k)]^2 / \sum_{k_0}^{k_1} k^5[\chi_{exptl}(k)]^2$$

with k = wave vector of the ejected photoelectron, $\chi(k)$ = EXAFS modulation of the absorption coefficient, $k_0 = 4$ Å^{-1}, and $k_1 = 11$ Å^{-1}.

The third peak exhibits a so-called focusing effect due to the fact that M, C, and O′ are almost aligned, as was already observed in $K_2Pt(C_2O_4)_2$.[11] (ii) If the stoichiometry of the compounds $CuNi(C_2O_4)_2$ is taken into account, the bridging network shown above is only compatible with a chain structure. The powder X-ray pattern excludes the presence of copper oxalate and strongly suggests an ordered structure deriving from the structure of nickel oxalate. Therefore, a 1/1 mixture of microcrystalline copper and nickel homometallic oxalates may be ruled out. A model consisting of alternating planes of ribbons of $Cu(C_2O_4)$ and $Ni(C_2O_4)$ could be consistent with EXAFS results. However, since the synthetic procedure is

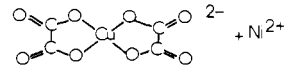

such a model appears quite unreasonable. We shall see further that both magnetic properties and EPR studies allow us to rule out this hypothesis. Consequently, the structure of ordered

(11) Teo, B. K. *J. Am. Chem. Soc.* **1981**, *103*, 3990.

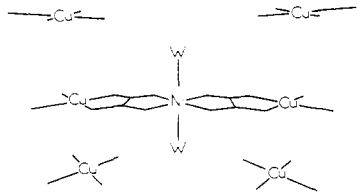

Figure 4. Proposed structure for bimetallic chain $CuNi(C_2O_4)_2 \cdot 4H_2O$.

bimetallic chains appears the most likely. (iii) At room temperature, only strongly correlated atomic positions can be seen, such as atoms in the same molecular entity. Intermolecular thermal vibrations corresponding to less strongly correlated movements disappear at 30 K. Therefore, the evolution of the spectra between 300 and 30 K allows us to distinguish between intra- and intermolecular distances, at least for heavy atoms.

For $Cu(C_2O_4) \cdot {}^1/_3H_2O$, at the Cu edge, the peak at 4.1 Å is quite intense at 30 K. It corresponds to four copper neighbors.[12] At the same distance, a less intense peak appears at 30 K for $CuNi(C_2O_4)_2 \cdot 4H_2O$, also at the Cu edge, which could be accounted for by one or two heavy atoms at about 4 Å from the copper. These heavy atoms can be identified as copper, given the absence of such a peak at this distance in the spectra at the Ni edge (see Figures 2 and 3).

Different models could fit the EXAFS results. Each copper atom has four oxygen atoms and each nickel atom has six oxygen atoms as nearest neighbors (Cu–O = 1.96 Å, Ni–O = 2.04 Å). Whereas Ni has only oxalato bridges and water molecules as visible EXAFS neighbors, Cu sees two other copper atoms situated at about 4 Å away and belonging to neighboring chains. The ordered bimetallic chain model, shown in Figure 4,is indeed the most likely model, if one takes into account all the experimental results. This structure is reminiscent of that of $CuMn(C_2O_2S_2)_2 \cdot 7.5H_2O$ determined by X-ray diffraction.[3] The discussion above holds for $Cu^{II}Zn^{II}$, with Zn replacing Ni and Zn–O = 2.08 Å.

Magnetic Properties

General Considerations. We considered a bimetallic ordered ring $(AB)_N$ with N AB units. A and B are magnetic ions without first-order angular momentum. Their spins are S_A and S_B, respectively, with $S_A \neq S_B$. Owing to the absence of first-order angular momentum, the interaction between nearest neighbors may be phenomenologically described by the Hamiltonian[13]

$$\mathcal{H} = -J\sum_{i=1}^{2N} \hat{S}_i \cdot \hat{S}_{i+1} \qquad (1)$$

with $\hat{S}_{2N+1} = \hat{S}_1$, and $\hat{S}_{2i-1} = \hat{S}_A$ and $\hat{S}_{2i} = \hat{S}_B$. If the interaction is antiferromagnetic, i.e. J negative, the level of lowest energy E_i has a spin $S_i = N(|S_A - S_B|)$. This corresponds to a ferrimagnetic-like chain with a sublattice $+NS_A$ and a sublattice $-NS_B$. The level of highest energy E_f has a spin $S_f = N(S_A + S_B)$. Between E_f and E_i, levels with spins inferior to S_i do exist, for instance with $S = 0$ if N is even or with $S = |S_A - S_B|$ if N is odd.

Let us examine how $\chi_M T$ varies vs. the temperature T, χ_M being the magnetic susceptibility per AB unit. At very high temperature, when $kT/|J|$ is very large, $\chi_M T$ tends to $(\chi_M T)^{HT}$, given by

$$(\chi_M T)^{HT} = \frac{N\beta^2 g^2}{3k}[S_A(S_A + 1) + S_B(S_B + 1)] \qquad (2)$$

in which it is assumed that the g_A and g_B local g factors have the same value g. At very low temperature, when $kT/|J|$ approaches zero, $\chi_M T$ tends to the limit

$$(\chi_M T)^{LT} = \frac{N\beta^2 g^2}{3k}[N(S_A - S_B)^2 + |S_A - S_B|] \qquad (3)$$

For

$$N_0 = \frac{S_A^2 + S_B^2 + 2S_<}{(S_A - S_B)^2}$$

where $S_<$ is the smaller of S_A and S_B, the limits $(\chi_M T)^{HT}$ and $(\chi_M T)^{LT}$ are equal. For $N > N_0$, $(\chi_M T)^{LT}$ is superior to $(\chi_M T)^{HT}$, and when N tends to the infinite, $(\chi_M T)^{LT}$ diverges. For $S_A = {}^1/_2$ and $S_B = 1$ ($Cu^{II}Ni^{II}$), N_0 is equal to 9. When cooling down the compound from a very high temperature, one depopulates first the level E_f, which has the highest spin. It results that $\chi_M T$ decreases. Therefore, one is led to the following general result: *For a chain of alternated and antiferromagnetically coupled spins S_A and S_B, $\chi_M T$ first decreases when the compound cools down, then reaches a minimum for a finite temperature, and finally diverges when the temperature approaches zero.*

If the interaction is ferromagnetic, i.e. J positive, the order of the spin levels is reversed with $S_i = N(S_A + S_B)$ and $S_f = N(|S_A - S_B|)$ and no extremum of the $\chi_M T$ vs. kT/J plot can be predicted a priori.

Calculations for the $(AB)_N$ Rings. We carried out the calculation of the magnetic behavior of $(AB)_N$ rings of alternated spins $S_A = {}^1/_2$ and $S_B = 1$, with $N = 2$–4, and we propose an extrapolation for $N \rightarrow \infty$. In the case $N = 2$, the spin levels can be obtained without any difficulty from the Hamiltonian (1) by using the vector model. On the other hand, for $(AB)_N$ with $N \geq 3$, it is necessary to use a numerical method. The Hamiltonian (1) is diagonalized by using as basis sets the microstates with M_S varying from 0 (if N is even) or ${}^1/_2$ (if N is odd) up to $N(S_A + S_B)$ successively. Such a method was used for the first time by Orbach in the case of a chain of spins ${}^1/_2$.[14] This leads to the energies of the spin levels and to their spin multiplicities. For $N = 3$, there are 48 levels, and for $N = 4$, 262 levels. The product $\chi_M T$ can be easily calculated from the spectrum of the spin levels $E_i(S)$ according to

$$\chi_M T = \frac{N\beta^2 g^2}{k} \frac{\sum_i \sum_{M_S=-S}^{M_S=+S} M_S^2 \exp[-E_i(S)/kT]}{\sum_i (2S + 1) \exp[-E_i(S)/kT]} \qquad (4)$$

The results are tabulated in the form of the variation of $\chi_M T(4/g^2)$ vs. $kT/|J|$. Table II corresponds to $J < 0$ and Table III to $J > 0$. For $J < 0$, all the curves have a minimum, which is more and more pronounced and displaced toward the large $kT/|J|$ when N increases. For $N = 2$, the minimum is obtained at $kT/|J| = 0.33$, for $N = 3$, at $kT/|J| = 0.47$, and for $N = 4$, at $kT/|J| = 0.55$. Above $kT/|J| = 0.7$, the curves meet very quickly, and for $kT/|J| \geq 1$, they are almost identical. For $J > 0$, $\chi_M T(4/g^2)$ continuously increases when $kT/|J|$ decreases, whatever N may be.

We propose an extrapolation for an infinite chain, by assuming a variation of $\chi_M T$ vs. the length N according to

$$\chi_M T = (\chi_M T)_\infty + a/N^\alpha$$

where a and α are coefficients depending on $kT/|J|$. The results of this extrapolation are given in the last column of Tables II and III. For the antiferromagnetic case ($J < 0$), the minimum is obtained for $kT/|J| = 0.63$ (8). For any

(12) Michalowicz, A.; Fourme, R. *Acta Crystallogr., Sect. A* 1981, *A37*, C307. Schmittler, H. *Monatsber. Dtsch. Akad. Wiss. Berlin* **1968**, *10*, 581.

(13) Girerd, J. J.; Charlot, M. F.; Kahn, O. *Mol. Phys.* **1977**, *34*, 1063.

(14) Orbach, R. *Phys. Rev.* **1959**, *115*, 1181.

Table II. $\chi_M T(4/g^2)$ vs. $kT/|J|$ for Antiferromagnetically Coupled $(AB)_N$ Ring Chains of Spins $S_A = 1/2$ and $S_B = 1$

	$\chi_M T(4/g^2)/(cm^3\ mol^{-1}\ K)$			
$kT/\|J\|$	$N=2$	$N=3$	$N=4$	$N\to\infty$
0	0.500 43	0.625 54	0.750 65	
0.05	0.500 43	0.625 54	0.750 65	
0.1	0.500 42	0.625 46	0.749 54	
0.15	0.500 22	0.624 08	0.741 47	
0.2	0.499 39	0.619 39	0.724 08	
0.25	0.497 96	0.611 46	0.700 76	
0.3	0.496 73	0.602 06	0.675 95	8.490
0.35	0.496 76	0.593 30	0.653 21	1.164 7
0.4	0.498 98	0.586 83	0.634 83	0.834 66
0.45	0.503 92	0.583 60	0.621 86	0.723 09
0.5	0.511 77	0.583 96	0.614 43	0.671 96
0.6	0.535 49	0.594 72	0.614 20	0.636 63
0.7	0.567 29	0.615 82	0.628 48	0.638 65
0.8	0.603 60	0.643 25	0.651 62	0.656 66
0.9	0.641 56	0.673 81	0.679 43	0.682 13
1	0.679 17	0.705 36	0.709 18	0.710 69
1.1	0.715 29	0.736 55	0.739 18	0.740 05
1.2	0.749 32	0.766 62	0.768 45	0.768 97
1.3	0.781 05	0.795 16	0.796 46	0.796 78
1.4	0.810 43	0.822 00	0.822 93	0.823 13
1.5	0.837 57	0.847 10	0.847 77	0.847 90
1.6	0.862 59	0.870 49	0.870 98	0.871 06
1.7	0.885 68	0.892 25	0.892 62	0.892 67
1.8	0.906 98	0.912 49	0.912 77	0.912 81
1.9	0.926 68	0.931 32	0.931 53	0.931 56
2	0.944 91	0.948 84	0.949 00	0.949 02
2.2	0.977 52	0.980 39	0.980 49	0.980 50
2.4	1.005 79	1.007 92	1.007 98	1.007 98
2.6	1.030 47	1.032 08	1.031 21	1.032 12
2.8	1.052 17	1.053 41	1.053 44	1.053 44
3	1.071 38	1.072 35	1.072 37	1.072 37
3.2	1.088 50	1.089 27	1.089 28	1.089 28
3.4	1.103 83	1.104 45	1.104 46	1.104 46
3.6	1.117 65	1.118 15	1.118 15	1.118 15
3.8	1.130 15	1.130 56	1.130 56	1.130 56
4	1.141 52	1.141 86	1.141 86	1.141 86

$kT/|J|$ above this value, the uncertainty of the extrapolated value of $\chi_M T$ is most likely less than 1%. This uncertainty is even negligible for $kT/|J| > 1$. In contrast, below the minimum of $\chi_M T$, in the range where $\chi_M T$ quickly diverges, the uncertainty may become much more important. That is why we do not give any extrapolated value for $kT/|J| < 0.3$. the exact curves for $N = 2$–4 and the extrapolated curve for $N \to \infty$ are shown in Figure 5a. The magnetic behavior for the infinite chain is represented again in Figure 5b in the form of $[\chi_M(4/g^2)(|J|/k)]^{-1}$ vs. $kT/|J|$. This representation puts into evidence that, in the range $1 \le kT/|J| \le 4$, the magnetic susceptibility very closely follows the empirical Curie–Weiss law:

$$\chi_M/(cm^3\ mol^{-1}) = 1.444(g^2/4)/(T/K + 1.0467|J|/k) \quad (5)$$

Calculated and extrapolated curves for the ferromagnetic case are shown in Figure 6.

Discussion of the Theoretical Results. In the discussion, we shall focus on the antiferromagnetic case. Before comparing the theoretical and the experimental data, it is quite important to specify clearly the theoretical frame in which the curves of Figures 5 and 6 and the expression (5) have been derived.

(i) We assumed that the local g factors were identical ($g_A = g_B = g$). This approximation may be criticized. As a matter of fact, we have shown recently that to obtain a good fitting of the magnetic properties for a $Cu^{II}Ni^{II}$ pair, it was important to take into account that g_{Cu} and g_{Ni} were different.[15] The complete calculation with $g_A \neq g_B$ is tedious since, in the presence of a magnetic field, the Zeeman perturbation couples the components of same M_S belonging to different spin states. We studied this effect in the $(AB)_2$ system. The results are shown in Figure 10.[26]

(ii) The B single-ion zero-field splitting ($S_B = 1$) has been neglected. Again the full calculation of the magnetic properties in the presence of local anisotropy is quite tedious, even if it does not present any conceptual difficulty. This has been made for the $(AB)_2$ system, and the results are represented in Figure 11.[26] As expected, the larger $|D|/|J|$ is, the more displaced is the minimum of $\chi_M T$ toward the lower temperatures.

(iii) We assumed that the interaction between nearest neighbors was purely isotropic. In fact, it is well-known that

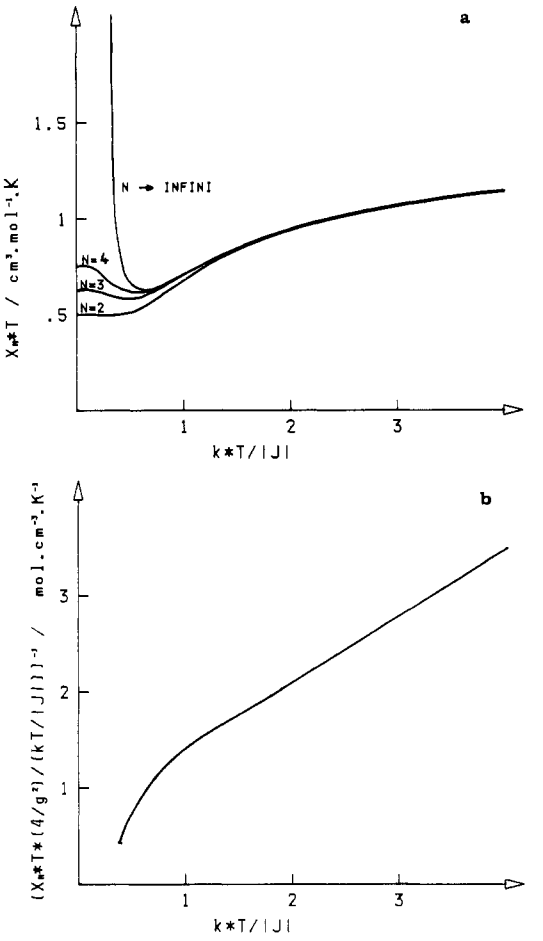

Figure 5. Magnetic behavior of antiferromagnetically coupled $(AB)_N$ ring chains of spins $S_A = 1/2$ and $S_B = 1$ (see text).

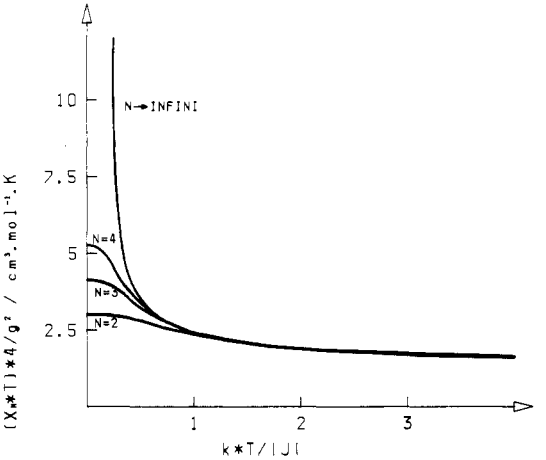

Figure 6. Magnetic behavior of ferromagnetically coupled $(AB)_N$ ring chains of spins $S_A = 1/2$ and $S_B = 1$ (see text).

(15) Morgenstern-Badarau, I.; Rerat, M.; Kahn, O.; Jaud, J.; Galy, J. *Inorg. Chem.* **1982**, *21*, 3050.

Table III. $\chi_M T(4/g^2)$ vs. $kT/|J|$ for Ferromagnetically Coupled $(AB)_N$ Ring Chains of Spins $S_A = 1/2$ and $S_B = 1$

	$\chi_M T(4/g^2)/(cm^3\ mol^{-1}\ K)$			
$kT/\|J\|$	$N = 2$	$N = 3$	$N = 4$	$N \rightarrow \infty$
0	3.002 59	4.128 56	5.254 53	
0.05	3.002 59	4.128 55	5.253 30	
0.1	3.002 54	4.124 28	5.196 19	
0.15	3.001 22	4.091 99	5.028 06	
0.2	2.995 23	4.018 25	4.785 08	
0.25	2.981 99	3.910 20	4.510 18	11.99
0.3	2.960 75	3.780 78	4.235 66	6.258
0.35	2.931 88	3.641 84	3.980 17	4.855 7
0.4	2.895 34	3.347 05	3.549 99	3.794 6
0.5	2.810 35	3.239 88	3.374 32	3.516 8
0.6	2.713 68	3.013 80	3.087 35	3.141 51
0.7	2.615 26	2.825 10	2.866 40	2.889 36
0.8	2.520 86	2.668 92	2.692 81	2.703 36
0.9	2.433 44	2.539 34	2.553 56	2.558 71
1	2.354 11	2.431 02	2.439 75	2.442 41
1.1	2.282 92	2.339 67	2.345 16	2.346 59
1.2	2.219 35	2.261 88	2.265 41	2.266 21
1.3	2.162 67	2.195 02	2.197 35	2.197 81
1.4	2.112 10	2.137 07	2.138 62	2.138 89
1.5	2.066 91	2.086 42	2.087 47	2.087 63
1.6	2.026 39	2.041 82	2.042 56	2.042 66
1.7	1.989 95	2.002 30	2.002 81	2.002 87
1.8	1.957 07	1.967 06	1.967 41	1.967 45
1.9	1.927 29	1.935 45	1.935 70	1.935 73
2	1.900 24	1.906 95	1.907 13	1.907 15
2.2	1.853 00	1.857 67	1.857 76	1.857 76
2.4	1.813 24	1.816 57	1.816 61	1.816 61
2.6	1.779 37	1.781 82	1.781 83	1.781 83
2.8	1.750 22	1.752 06	1.752 06	1.752 06
3.0	1.724 90	1.726 30	1.726 30	1.726 30
3.2	1.702 71	1.703 80	1.703 80	1.703 80
3.4	1.683 12	1.683 98	1.683 98	1.683 98
3.6	1.665 71	1.666 40	1.666 40	1.666 40
3.8	1.650 14	1.650 69	1.650 69	1.650 69
4.0	1.636 13	1.636 58	1.636 58	1.636 58

the single-ion spin–orbit coupling may lead possibly to a small anisotropic exchange contribution. Its effect is analogous to that of the local anisotropy of the B ions studied above.[15,16]

(iv) Finally, our theoretical approach deals with perfectly isolated $(AB)_N$ chains. In fact, much above the critical temperature where a three-dimensional order appears, the interchain interactions may substantially modify the magnetic behavior in the range of the low temperatures. A quantitative investigation of this effect cannot be performed in the absence of information on the exchange pathways between ions belonging to different chains. Nevertheless, it is clear that, if the interchain interactions are antiferromagnetic, as is most often the case, the minimum of the $\chi_M T$ vs. T plot is displaced toward the low temperatures and eventually may not be detectable.

To conclude this section, we can notice that the local anisotropy around the B ions, the anisotropic exchange, and interchain interactions of antiferromagnetic nature all have as a consequence the shifting of the minimum of the $\chi_M T$ vs. T plot toward the low temperatures. In other respects, any breaking in the chain will have as a consequence the diminishing of the correlation length, so that the $\chi_M T$ values for the lowest temperatures will be lessened.

Experimental Results. The magnetic behavior of the $Cu^{II}Ni^{II}$ compound is shown in Figure 7. From Figure 7, one sees that $\chi_M T$ continuously decreases when the system is cooled down, from 1.33 $cm^3\ mol^{-1}\ K$ at 295 K to 0.152 $cm^3\ mol^{-1}\ K$ at 1.81 K. Therefore, $\chi_M T$ does not present the minimum expected from the theory. Figure 7 shows that, above 30 K,

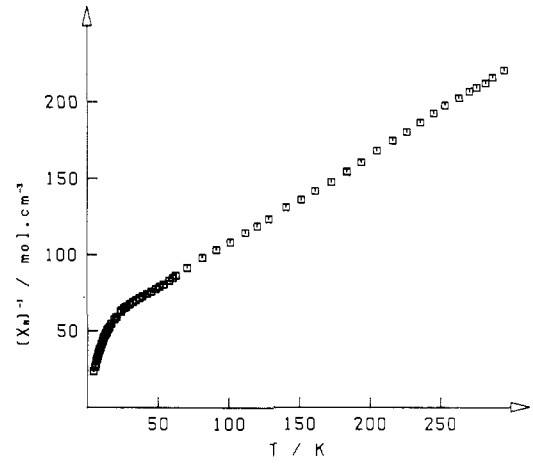

Figure 7. Magnetic behavior of $CuNi(C_2O_4)_2 \cdot 4H_2O$: (□) experimental data; (—) theoretical curve (see text).

the experimental magnetic susceptibility follows the Curie–Weiss law $\chi_M/(cm^3\ mol^{-1}) = 1.689/(T/K + 79.4)$. By comparing this experimental expression to the theoretical one (5), one obtains

$$J = -52.7\ cm^{-1} \qquad g = 2.162$$

The problem at hand is why, in the present case, the minimum of $\chi_M T$ is not observed. From the Hamiltonian (1) with $J = -52.7\ cm^{-1}$, this minimum was expected at 49 K. Since the interaction is large, the ratio $|D|/|J|$ where D is due to both local anisotropy and anisotropic exchange is likely much too weak to account for the absence of a minimum. On the other hand, we have seen in the section on structure that each Cu^{II} ion "saw" two other Cu^{II} ions belonging to other chains and located at 4 Å. This might provide a relatively efficient interchain exchange pathway. This hypothesis is backed by the study of the magnetic properties of $CuZn(C_2O_4)_2 \cdot 4H_2O$. The shortest intramolecular Cu···Cu distance through the Cu-$(C_2O_4)Zn(C_2O_4)$Cu network in an ordered bimetallic chain is around 10.3 Å, so that the intramolecular interaction is negligible. From the empirical relation proposed by Coffman and Buettner,[17] providing the largest antiferromagnetic interaction for a given Cu···Cu separation, J would be less than 0.12 cm^{-1}. As expected for a noncoupled Cu^{II} compound, $\chi_M T$ is nearly constant when the system is cooled down from room temperature to about 100 K and equal to 0.38 $cm^3\ mol^{-1}\ K$, but below 100 K, $\chi_M T$ decreases to 0.20 $cm^3\ mol^{-1}\ K$ at 2 K. This behavior, which does not correspond at all to the law for a chain of spins $1/2$, may be explained only by the interchain interactions. It should be recalled here that the magnetic behavior of $Cu(C_2O_4) \cdot {}^1/_3H_2O$, characteristic of a chain with a large intrachain antiferromagnetic coupling, is totally different from that of $CuZn(C_2O_4)_2 \cdot 4H_2O$.[19]

The EPR spectrum of $CuZn(C_2O_4)_2 \cdot 4H_2O$ shown in Figure 8b is also interesting in that it is characteristic of an noncoupled Cu^{II} ion in an axially elongated surrounding, with $g_\parallel = 2.25$ (6) and $g_\perp = 2.11$ (7). It completely differs from the EPR spectrum of $Cu(C_2O_4) \cdot {}^1/_3H_2O$ shown in Figure 8a, which reveals magnetically nonequivalent chains[18] with effective values $g_\parallel = 2.08$ (7) and $g_\perp = 2.21$ (6). The $Cu^{II}Ni^{II}$ chain does not exhibit any EPR signal in the 4.2–300 K temperature range. The reasons the $Cu^{II}Ni^{II}$ chain behaves like this are not clear to us. However, the absence of an EPR signal confirms, if it was still necessary, that in this compound there is neither isolated Cu^{II} ions nor Cu^{II} clusters, which is con-

(16) Banci, L.; Bencini, A.; Dei, A.; Gatteschi, D. *Inorg. Chem.* **1981**, *20*, 393.

(17) Coffman, R.; Buettner, G. R. *J. Phys. Chem.* **1979**, *83*, 2387.
(18) McGregor, K. T.; Soos, Z. G. *Inorg. Chem.* **1976**, *15*, 2159.

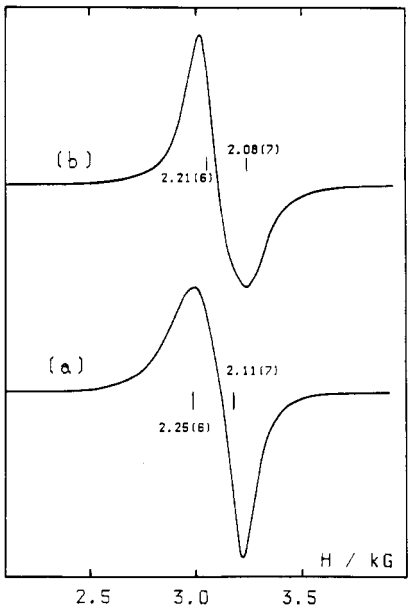

Figure 8. X-band EPR spectra of (a) $CuZn(C_2O_4)_2 \cdot 4H_2O$ and (b) $Cu(C_2O_4) \cdot {}^1/_3H_2O$.

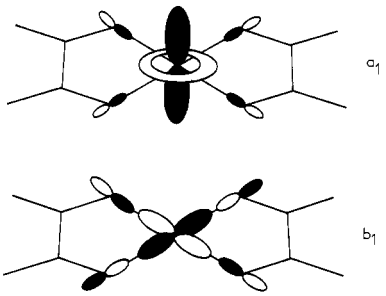

Figure 9. a_1 and b_1 magnetic orbitals in μ-oxalato-bridged chains.

sistent of course with the ordered bimetallic structure.

Conclusion

In this last section, we propose to approach briefly two problems, namely the comparison of the bimetallic $Cu^{II}Ni^{II}$ chain with the homometallic copper oxalate and nickel oxalate, and the problem of the low-temperature magnetic behavior.

In $Cu(C_2O_4) \cdot {}^1/_3H_2O$, J_{CuCu} is -291 cm^{-1}.[19] We redetermined accurately J_{NiNi} in $Ni(C_2O_4) \cdot 2H_2O$ and found it to be -24.1 cm^{-1},[20] a value close to the one obtained by Reedijk et al.[21] J_{CuNi} in $CuNi(C_2O_4)_2 \cdot 4H_2O$ has a value intermediate between J_{CuCu} and J_{NiNi}. The J_{AB} parameters may be expressed as sums of contributions involving pairs of magnetic orbitals according to

$$J_{CuCu} = J_{b_1b_1} = -291 \text{ cm}^{-1}$$
$$J_{NiNi} = {}^1/_4(J_{b_1b_1} + J_{a_1a_1} + 2J_{a_1b_1}) = -24.1 \text{ cm}^{-1} \quad (6)$$
$$J_{CuNi} = {}^1/_2(J_{b_1b_1} + J_{a_1b_1}) = -52.7 \text{ cm}^{-1}$$

where the a_1 and b_1 magnetic orbitals are schematized in Figure 9. From (6), we could extract the set of parmeters $J_{b_1b_1} = -291$ cm^{-1}, $J_{a_1a_1} = -176.6$ cm^{-1}, and $J_{a_1b_1} = 185.6$ cm^{-1}. The values have the proper sign and the good relative energies. Indeed, owing to the out-of-bond oxygen–oxygen overlap, $J_{b_1b_1}$ is expected to be strongly negative.[22] $J_{a_1a_1}$ involving magnetic orbitals more weakly delocalized toward the oxalato bridges is expected to be less negative, and $J_{a_1b_1}$ is certainly positive since the involved magnetic orbitals are orthogonal.[23] However, the meaning of this unique set of parameters appears to us uncertain. Nothing justifies, for instance, that $J_{b_1b_1}$ is invariant in the three compounds. It was already noticed that the b_1 exchange pathway had a quite specific efficiency in planar

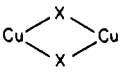

networks[24] and in the $Cu(C_2O_4)Cu$ network.[22] In this respect, one can notice that the Ni–O bonds (2.04 Å) are significantly longer than the Cu–O bonds (1.96 Å); the b_1 magnetic orbital may be more delocalized on the oxygen bridging atoms for Cu^{II} than for Ni^{II}.

As for the magnetic behavior of the ordered bimetallic chains in the low-temperature range, it remains an open problem. Systems of this kind were synthesized in other groups; the $\chi_M T$ vs. T plots exhibit no minimum.[25] The question at hand is "can this minimum be observed and, if not, why?" Particularly interesting, in this respect, would be bimetallic chains well isolated from each other with a strong intrachain isotropic coupling. Our group is working in this direction.

Acknowledgment. We are most grateful to Dr. Marin and his colleagues of the Laboratoire de l'Accelerateur Linéaire d'Orsay for the operation of the storage ring DCI, to Drs. Lagarde and Sadoc for the access to the EXAFS I spectrometer of LURE, to the staff of LURE, to Dr. Goulon for his help in programming, and to Prof. Fourme for helpful discussions.

Registry No. $CuNi(C_2O_4)_2 \cdot 2H_2O$, 86527-36-8; $CuZn(C_2O_4)_2 \cdot 2H_2O$, 86527-38-0.

Supplementary Material Available: Graphs of the influence of $K = g_B/g_A$ (Figure 10) and of $D/|J| = \pm 0.1$ (Figure 11) on the magnetic behavior of $(AB)_2$ with $J < 0$ (2 pages). Ordering information is given on any current masthead page.

(19) Girerd, J. J.; Verdaguer, M.; Kahn, O. *Inorg. Chem.* **1980**, *19*, 274.
(20) Unpublished result.
(21) Van Kralingen, C. G.; Van Ooijen, J. A. C.; Reedijk, J. *Transition Met. Chem. (Weinheim, Ger.)* **1978**, *3*, 90.
(22) Julve, M.; Verdaguer, M.; Kahn, O.; Gleizes, A.; Philoche-Levisalles, M. *Inorg. Chem.* **1983**, *22*, 368.
(23) Kahn, O.; Galy, J.; Journaux, Y.; Jaud, J.; Morgenstern-Badarau, I. *J. Am. Chem. Soc.* **1982**, *104*, 2165.
(24) Lambert, S. L.; Spiro, C. L.; Gagne, R. R.; Hendrickson, D. N. *Inorg. Chem.* **1982**, *21*, 68.
(25) Drillon, M., private communication.
(26) Supplementary material.